Fetal Leydig Cells Persist as an Androgen-Independent Subpopulation in the Postnatal Testis

Yuichi Shima,* Sawako Matsuzaki,* Kanako Miyabayashi, Hiroyuki Otake, Takashi Baba, Shigeaki Kato, Ilpo Huhtaniemi, and Ken-ichirou Morohashi

Department of Molecular Biology (Y.S., S.M., K.M., H.O., T.B., K.-i.M.), Graduate School of Medical Sciences, Kyushu University, Fukuoka 812-8582, Japan; Soma Central Hospital (S.K.), Soma, Fukushima 976-0016, Japan; Institute of Reproductive and Developmental Biology (I.H.), Department of Surgery and Cancer, Imperial College London, London W12 0NN, United Kingdom; and Department of Physiology (I.H.), University of Turku, 20520 Turku, Finland

Two distinct types of Leydig cells emerge during the development of eutherian mammals. Fetal Leydig cells (FLCs) appear shortly after gonadal sex differentiation, and play a crucial role in masculinization of male fetuses. Meanwhile, adult Leydig cells (ALCs) emerge after birth and induce the secondary male-specific sexual maturation by producing testosterone. Previous histological studies suggested that FLCs regress completely soon after birth. Furthermore, gene disruption studies indicated that androgen signaling is dispensable for FLC differentiation but indispensable for postnatal ALC differentiation. Here, we performed lineage tracing of FLCs using a FLC enhancer of the *Ad4BP/SF-1* (*Nr5a1*) gene and found that FLCs persist in the adult testis. Given that postnatal FLCs expressed androgen receptor (AR) as well as LH receptor (LuR), the effects of AR disruption on FLCs and ALCs were analyzed by crossing AR knockout (KO) mice with FLC-specific enhanced green fluorescent protein (EGFP) mice. Moreover, to eliminate the influence of elevated LH levels in ARKO mice, LuRKO mice and AR/LuR double-KO mice were analyzed. The proportion of ALCs to postnatal FLCs was decreased in ARKO mice, and the effect was augmented in the double-KO mice, suggesting that androgen signaling plays important roles in ALCs, but not in FLCs. Finally, ARKO was achieved in an FLC-specific manner (FLCARKO mice), but the FLC number and gene expression pattern appeared unaffected. These findings support the conclusion that FLCs persist as an androgen-independent Leydig subpopulation in the postnatal testis. (*Molecular Endocrinology* 29: 1581–1593, 2015)

Leydig cells are localized in the interstitial space of the testis and play essential roles in masculinization of the whole body by producing androgens. It has been described that eutherian mammals have 2 different types of Leydig cells: fetal Leydig cells (FLCs) and adult Leydig cells (ALCs) (1, 2). In mice, FLCs appear in the fetal testis at embryonic day (E) 12.5 and increase in number during fetal life. FLCs express steroidogenic enzymes required for androgen synthesis, such as steroidogenic acute regulatory protein, CYP11A1 (P450 side chain cleavage), CYP17A1 (P450C17), and 3β-hydroxysteroid dehydro-

genase type 1, but do not express 17β-hydroxysteroid dehydrogenase type 3 (HSD17B3), an enzyme mediating the final reaction for testosterone synthesis. Therefore, the major androgen produced by FLCs is androstenedione, which is then converted to testosterone by HSD17B3 expressed in fetal Sertoli cells (3, 4). On the other hand, ALCs start to develop at around 1 week after birth and rapidly increase in number during pubertal progression. ALCs become functionally mature at 40 days after birth (5). They express HSD17B3 as well as other steroidogenic enzymes, and are thus capable of synthesizing testoster-

one by themselves. Massive testosterone production by ALCs is essential for the development of male-specific secondary sex characteristics.

It has generally been believed that FLCs completely disappear and ALCs newly develop after birth, and most studies on Leydig cells to date have been performed on the basis of this assumption (1, 2, 6–9). On the contrary, a few papers have argued for the persistence of FLCs in the postnatal testis (10, 11). However, both claims were mainly based on morphological observations of fetal and postnatal testes, and the fate of FLCs has remained controversial.

Testosterone exerts its functions by binding to its receptor, androgen receptor (AR) (officially NR3C4). Therefore, the functional importance of androgen signaling has been verified by generating *Ar* gene knockout (KO) mice. FLCs developed normally in the ARKO mouse fetal testis, and the testes of ARKO mice appeared normal until postnatal day (P) 5, suggesting that FLCs develop in an androgen-independent manner. Thereafter, the postnatal testicular development was largely impaired in ARKO mice. Specifically, the testes remained quite small compared with those in wild-type mice, the seminiferous tubules remained narrow probably through spermatogenic arrest, and the interstitial cells appeared hyperplastic (12, 13). Intriguingly, the Leydig cells in adult ARKO mice did not express ALC marker proteins, such as HSD17B3 and 3β-hydroxysteroid dehydrogenase type 6 (HSD3B6) (13). Because FLCs are believed to disappear after birth, the Leydig cells in ARKO mice were considered to be immature ALCs. However, as FLCs are also negative for HSD3B6 and HSD17B3, it was difficult to conclude whether the Leydig cells in the ARKO mouse testis were FLCs or immature ALCs.

LH secreted from the pituitary gonadotropes plays an essential role in postnatal Leydig cell development. Indeed, LHβKO mice showed decreased testes size, hypoplastic Leydig cells, and reduced testosterone levels at adult stage (14). LH receptor (LuR) expression is detectable in FLCs from E16 onwards (15), and fetal testes respond to LH stimulation with increased testosterone production (16). However, the neonatal LuRKO testes are indistinguishable from wild-type testes, indicating that although FLC are LH responsive, they are not LH dependent. In contrast, the testes of adult LuRKO mice were significantly underdeveloped and contained fewer and hypotrophic Leydig cells, strongly suggesting that LH signaling is essential for Leydig cell development at postnatal stages (9, 17–19).

Previously, we identified a FLC enhancer (FLE) of the *Ad4BP/SF-1* (*Nr5a1*) gene (20) and generated transgenic mice in which FLCs are labeled with enhanced green fluorescent protein (EGFP) (*SmAc1.8-Ad4BP(LBmut)-EGFP* mice, here designated as *mFLE-EGFP* mice) (4). As a consequence of EGFP expression in both the fetal and adult testes of these mice, it was suggested that FLCs persist in the postnatal testis. In the present study, we initially compared the expressions of EGFP and the ALC marker enzymes HSD3B6 and HSD17B3 in *mFLE-EGFP* mice. Immunofluorescence analyses revealed that most EGFP-positive cells were negative for HSD3B6 and HSD17B3 in both the fetal and adult testes, suggesting that FLCs persist after birth. Moreover, we performed lineage-tracing experiments of FLCs and confirmed that FLCs and/or their descendants existed in the adult testis. Because FLCs were proven to persist after birth, we investigated the expressions of AR and LuR in FLCs at prenatal and postnatal stages. AR was expressed in postnatal FLCs, but not in prenatal FLCs, whereas LuR was expressed in FLCs from fetal to adult stages. We further investigated the functional importance of AR and LuR in FLCs and ALCs by crossing *mFLE-EGFP* mice with ARKO, LuRKO, and AR/LuR double-KO (DKO) mice. The results of cell counting analyses strongly suggested that androgen signaling is indispensable for ALC development, but dispensable for postnatal FLCs. Finally, the cell-autonomous functions of androgen signaling in FLCs were investigated by generating FLC-specific ARKO (FLCARKO) mice. These mice showed normal testosterone levels, normal reproductive tissues, and normal reproductive performance. Based on the above results, we conclude that FLCs persist as an androgen-independent Leydig subpopulation in the postnatal testis.

Materials and Methods

Mice

We previously reported that *mFLE-EGFP* mice specifically express EGFP in FLCs (4). Two transgene constructs, *mFLE-Cre* and *mFLE-CreERT2*, were generated by replacing *EGFP* in *mFLE-EGFP* with *Cre* and *CreERT2*, respectively. The presence of the appropriate transgene in *mFLE-Cre* and *mFLE-CreERT2* mice was examined by PCR using the next primers that amplify both *Cre* and *CreERT2*: 5′-GCGGCATGGTG-CAAGTTGAAT-3′ and 5′-ACCCCCAGGCTAAGTGCCTT-3′. For lineage-tracing experiments, *mFLE-CreERT2* mice were crossed with *CAG-CAT-EGFP* mice (21), and 100-mg/kg body weight of tamoxifen (Sigma) dissolved in corn oil containing 10% ethanol was administered ip to pregnant females at E14.5. EGFP expression was observed at E18.5 and P56. To investigate the roles of AR and LuR in FLCs and ALCs, ARKO (22), LuRKO (17), and AR/LuR-DKO mice harboring the *mFLE-EGFP* transgene were generated. FLCARKO mice were generated by mating *mFLE-Cre* mice with AR-flox mice (23). To reveal the fate of FLCs in FLCARKO mice, FLCARKO mice harboring the *CAG-CAT-EGFP* transgene were also generated.

Mice were euthanized under deep anesthesia with sevoflurane (Maruishi Pharmaceutical Co Ltd). All protocols for animal experiments were approved by the Animal Care and Use Committee of Kyushu University (permission number A26–001).

Immunofluorescence analyses

For immunofluorescence analyses, testes collected at E18.5, P10, and P21 were immersion fixed in 4% paraformaldehyde (PFA) at 4°C for 48 hours. In addition, P56 mice were perfused with 4% PFA, and their testes were collected and immersion fixed in 4% PFA at 4°C for 48 hours. The specimens were subsequently soaked in 20% sucrose at 4°C for 24 hours and embedded in OCT Compound (Sakura Finetek). Immunofluorescence analyses were performed as previously described (24). Briefly, cryosections (10-μm thickness) were boiled in 10mM sodium citrate (pH 6.0) to unmask antigen epitopes. The primary and secondary antibodies used in this study are listed in Supplemental Table 1. Can Get Signal Solution A (Toyobo) was used for HSD3B6 and HSD17B3 staining to enhance the immunofluorescence. 4′6′-diamidino-2-phenylindole (Sigma) was used for nuclear staining. Immunofluorescence was detected using a BZ-9000 microscope (Keyence) or an LSM700 confocal microscope (Carl Zeiss).

Immunoelectron microscopy

Adult *mFLE-EGFP* mice (n = 3) were transcardially perfused with PBS, followed by 4% PFA and 0.5% glutaraldehyde in PBS. The testes were collected, immersion fixed in the same fixative for 16 hours, washed with PBS several times, and postfixed with 1% osmium tetroxide and 0.75% potassium ferrocyanide. The specimens were then dehydrated through increasing concentrations of ethanol, embedded in LRW Resin (Electron Microscopy Sciences) in gelatin capsules, and polymerized under UV lamps at −20°C overnight. Ultrathin sections (100- to 120-nm thickness) were collected on nickel grids covered with plastic film, incubated in 3.8% sodium iodate for 1 hour at room temperature, washed with distilled water several times, and incubated with 2% BSA in PBS for 30 minutes at room temperature. Subsequently, the sections were incubated with a 1:10 dilution of a rabbit antibody against EGFP (Living Colors Av Peptide Antibody 632377; Clontech Laboratories) at 4°C overnight, washed with PBS, and incubated with a 1:100 dilution of Immunogold EM Goat Antirabbit IgG (BBI Solutions) for 3 hours at room temperature. Finally, the sections were contrasted with 0.2% tannic acid solution, uranyl acetate, and lead citrate, and viewed with an H-7600 electron microscope (Hitachi).

Cell sorting and quantitative RT-PCR (qRT-PCR)

EGFP-positive FLCs were collected from E18.5, P10, P21, and P56 testes by fluorescence-activated cell sorting as previously described (4). ALCs were collected from P56 wild-type testes by Percoll density gradient centrifugation as previously described (4). Total RNA was isolated from each sample, and subjected to qRT-PCR. Briefly, total RNA was isolated from the cells using an RNeasy Micro kit (QIAGEN GmbH) and subjected to reverse transcription with SuperScript II Reverse Transcriptase (Life Technologies). Quantitative PCR was performed with an ABI 7500 Real-Time PCR System (Applied Biosystems) using THUNDERBIRD SYBR qPCR Mix (Toyobo). The gene expression levels were standardized by the β-actin (*Actb*) gene expression levels. The primers used for PCR are listed in Supplemental Table 2.

Cell counting

Three specimens from individual mice were prepared for each experimental group, and the testes were sectioned and stained with the antibodies against EGFP. The numbers of cells were counted in 25 nonoverlapping views (1 view = 0.48 mm^2), and the cell number per unit area (cells/mm^2) was calculated.

Measurement of intratesticular testosterone

Three testes from control and FLCARKO mice (n = 3 for each) were collected at P56 and stored at −80°C until analysis. The concentrations of intratesticular testosterone were determined by LC-MS/MS (ASKA Pharma Medical Co Ltd).

Hematoxylin and eosin (H&E) staining

Testes were collected from control and FLCARKO mice (n = 3 for each) at P56, fixed with Bouin's solution at 4°C for 24 hours, and embedded in paraffin wax. The tissues were sectioned at 5-μm thickness and subjected to H&E staining.

Fertility test

Male control and FLCARKO mice (n = 3 for each) at P56 and P105 were evaluated for fertility. After single C57BL/6 female mice were mated with the male mice for 4 days, the female mice were separated until delivery. The procedure was continuously repeated, such that 3 females were used for each male.

Statistical analysis

At least 3 animals for each experimental group were used in all experiments, and the qRT-PCR analyses were performed in triplicate. Data are presented as mean ± SEM. Differences between experimental groups were examined by a 2-tailed Student's t test, and statistical significance was determined by values of $P < .05$.

Results

FLCs persist in the postnatal testis as a subpopulation of Leydig cells

In our previous study, we identified an FLE in the *Ad4BP/SF-1* (*Nr5a1*) gene (20) and generated a transgenic mouse line in which FLCs are labeled with EGFP (*mFLE-EGFP* mice) (Figure 1A) (4). Immunofluorescence staining revealed that marker proteins for Leydig cells, Ad4BP/SF-1 and HSD3B, were expressed in the EGFP-labeled cells in both the fetal and adult testes (Figure 1, B–E). There are 7 HSD3B isoforms in mice, and previous studies showed that HSD3B6 is expressed in ALCs, but not in FLCs (4, 5). Given that our polyclonal antibody was originally raised against 3β-hydroxysteroid dehydrogenase type 1 (25), which is expressed in both FLCs and ALCs, we used a recently generated HSD3B6-
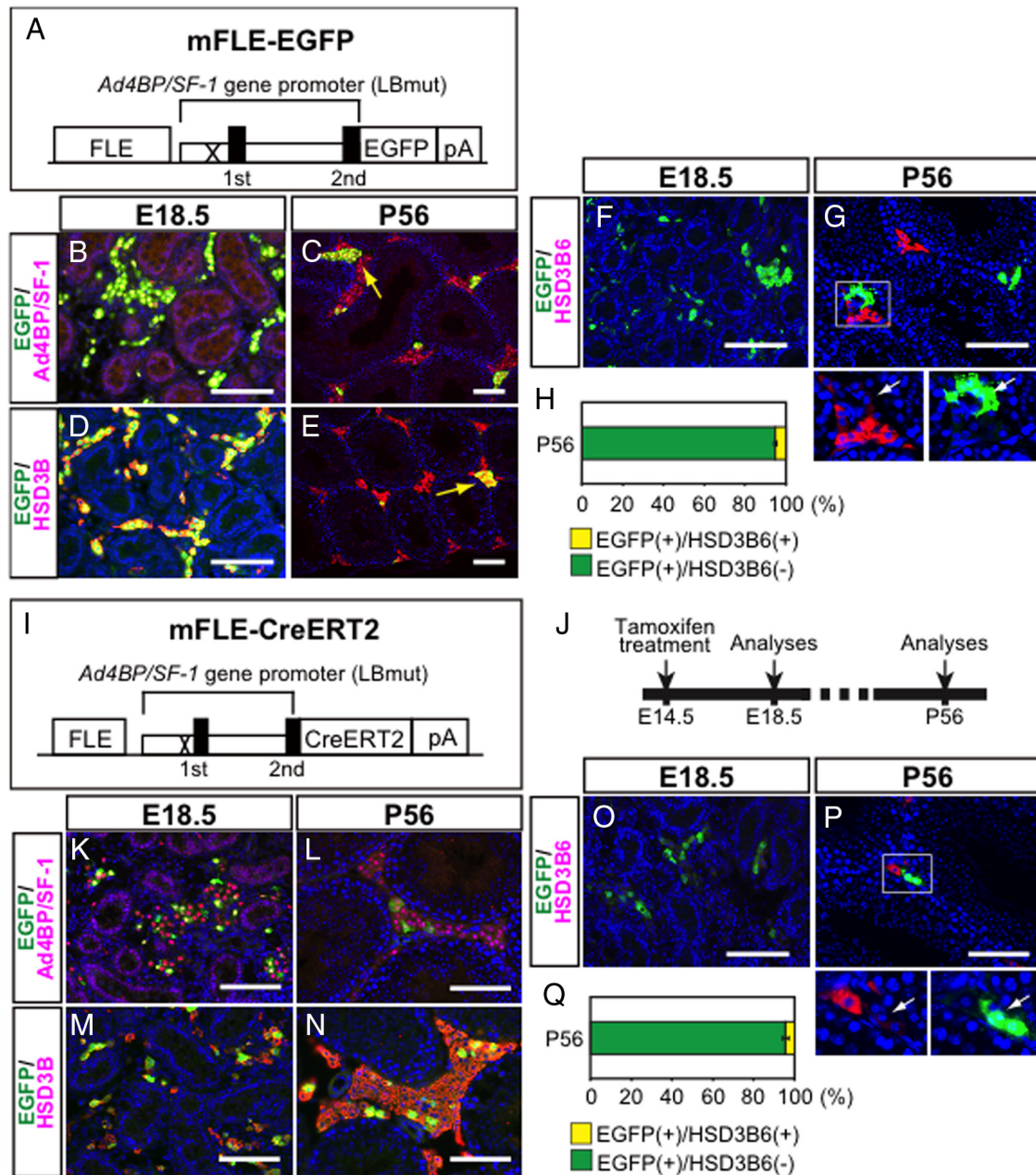
Figure 1. Lineage tracing of FLCs. A, Schematic diagram of the transgenic construct, *mFLE-EGFP*, designed to express *EGFP* specifically in FLCs. An LHX9-binding site in the proximal promoter of the *Ad4BP/SF-1* gene was mutated (X). The closed boxes indicate the first and second exons. pA, poly(A) signal. B–E, Testicular sections at E18.5 (B and D) and P56 (C and E) were stained with antibodies recognizing EGFP (green) and Ad4BP/SF-1 (red) (B and C), or EGFP (green) and HSD3B (red) (D and E). Arrows indicate double-positive cells. F and G, Testicular sections at E18.5 (F) and P56 (G) were stained with antibodies recognizing EGFP (green) and HSD3B6 (red). The area enclosed by the rectangle in G was enlarged, and the signals in each channel are shown in the small panels. Arrows indicate EGFP(+) and HSD3B6(−) cells. H, The ratio between EGFP(+)/HSD3B6(−) and EGFP(+)/HSD3B6(+) cells in P56 testes is shown as mean ± SEM. I, Schematic diagram of the transgenic construct, *mFLE-CreERT2*, designed to express *CreERT2* specifically in FLCs. J, To study the FLC lineage, *mFLE-CreERT2;CAG-CAT-EGFP* mice were treated with tamoxifen at E14.5 and then analyzed at E18.5 and P56. K–N, Testicular sections at E18.5 (K and M) and P56 (L and N) were stained with antibodies recognizing EGFP (green) and Ad4BP/SF-1 (red) (K and L), or EGFP (green) and HSD3B (red) (M and N). O and P, Testicular sections at E18.5 (O) and P56 (P) were stained with antibodies recognizing EGFP (green) and HSD3B6 (red). The area enclosed by the rectangle in P was enlarged, and the signals in each channel are shown in the small panels. Arrows indicate EGFP(+) and HSD3B6(−) cells. Q, The ratio between EGFP(+)/HSD3B6(−) and EGFP(+)/HSD3B6(+) cells in P56 testes is shown as mean ± SEM. Scale bars,100 µm.

specific antibody (26) to examine whether the EGFP-labeled Leydig cells were of the fetal or adult type. As expected, HSD3B6 expression was not detected in the fetal testis (Figure 1F). On the other hand, approximately 95%

of the EGFP-positive cells were negative for HSD3B6 in the adult testis (Figure 1, G and H). In addition, the EGFP-positive cells were mostly negative for another ALC marker protein, HSD17B3 (Supplemental Figure 1).

Because FLCs appeared to occupy a small percentage of total Leydig cells in the adult testis, we examined proliferative activity in FLCs. Immunofluorescence analyses with the antibodies against EGFP and phospho-histone H3 revealed that EGFP signals hardly overlapped with phospho-histone H3 signals in *mFLE-EGFP* testes at E18.5 and P56 (Supplemental Figure 2), indicating that FLCs are not actively proliferating both at fetal and adult stages. It was reported that lipid droplets were more abundant in FLCs than ALCs (10, 11). Therefore, immunoelectron microscopy analyses were performed to reveal the microstructures in EGFP-positive and EGFP-negative cells. However, the abundance of lipid droplets did not appear to differ between EGFP-positive and EGFP-negative cells, and no obvious differences were observed between the 2 cell populations (Supplemental Figure 3). Although immunofluorescence staining strongly suggested that FLCs persisted in the adult testis, it remained unclear whether they were descendants of FLCs from the fetal testis. To address this possibility, we performed lineage-tracing experiments. Mice specifically expressing *Cre-ERT2* in FLCs were generated using the transgenic construct *mFLE-CreERT2* (Figure 1I) and then crossed with *CAG-CAT-EGFP* mice (21). The pregnant females were treated with tamoxifen at E14.5 to trace FLCs (Figure 1J). FLCs were successfully labeled with EGFP in the E18.5 testis (Figure 1, K and M), although the labeling efficiency was less than 50% (Supplemental Figure 4). In the adult testis, EGFP-labeled cells persisted in the interstitium, and were positive for Ad4BP/SF-1 and HSD3B (Figure 1, L and N), indicating that FLCs and/or their descendants persist in the adult testis. None of the EGFP-labeled cells expressed HSD3B6 in the fetal testis (Figure 1O), and approximately 95% of the EGFP-labeled cells were HSD3B6-negative in the adult testis (Figure 1, P and Q). In addition, EGFP-positive cells mostly contributed to the HSD17B3-negative cell population, although a small number of EGFP/HSD17B3-double-positive cells were observed (Supplemental Figure 5). Taken together, these data indicated that FLCs persisted as an HSD3B6-negative subpopulation of Leydig cells even in the adult testis, although the existence of EGFP/HSD3B6-double-positive cells (~5% of total EGFP-labeled cells) observed in the lineage-tracing experiments leaves open the possibility that a small portion of FLCs transdifferentiated into ALCs.

Expressions of AR and LuR in FLCs

The expression of AR in FLCs was examined by immunofluorescence staining. At E18.5, AR was expressed in interstitial cells, including peritubular myoid cells and mesenchymal cells (Figure 2A). However, the AR signals
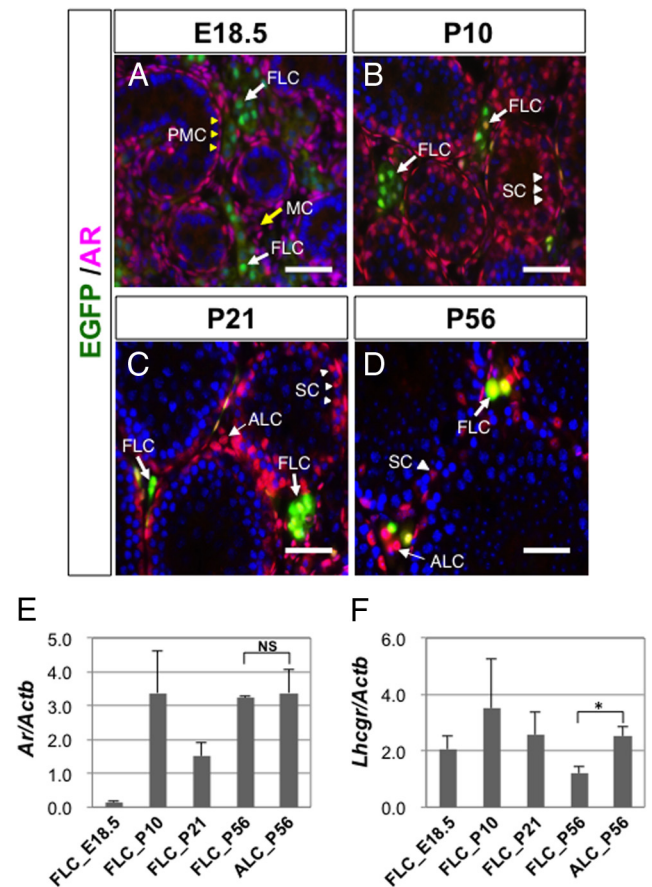
Figure 2. AR and LuR expressions in FLCs. A–D, Testes were collected from wild-type mice at E18.5, P10, P21, and P56 and subjected to immunofluorescence analyses with antibodies against EGFP (green) and AR (red). EGFP-positive FLCs are indicated by bold arrows in A–D, whereas EGFP-negative interstitial cells (putative ALCs) are indicated by thin arrows in C and D. The peritubular myoid cells (PMCs) and mesenchymal cells (MCs) in the fetal testis are indicated by yellow arrowheads and yellow arrows in A, respectively. Sertoli cells (SCs) are indicated by arrowheads in B–D. Scale bars, 50 μm. E and F, FLCs were collected from *mFLE-EGFP* mouse testes at E18.5, P10, P21, and P56 by cell sorting, and the expression levels of *Ar* and *Lhcgr* were measured by qRT-PCR. ALCs were collected from P56 wild-type testes by Percoll density gradient centrifugation and also subjected to the analyses. The expression levels of *Ar* and *Lhcgr* were standardized by the β-actin (*Actb*) expression levels. The data are shown as mean ± SEM. *, $P < .05$, significant difference. NS, no significant difference.

never overlapped with the EGFP signals at this stage. These findings were consistent with previous reports showing that prenatal FLCs are negative for AR (27, 28), although AR expression was detectable in rat FLCs after E21 (29). At P10, AR was strongly expressed in peritubular myoid cells, and also expressed in Sertoli cells. In addition, AR signals were detected in a part of the EGFP-positive FLCs, although the expression levels varied, with some cells appearing AR-negative and others appearing weakly or fairly positive for AR (Figure 2B). AR expression was detected in nearly all FLCs as well as in all ALCs (EGFP-negative Leydig cells) at P21 and P56 (Figure 2, C

and D). In these stages, AR expression continued in peritubular myoid cells and Sertoli cells (Figure 2, C and D).
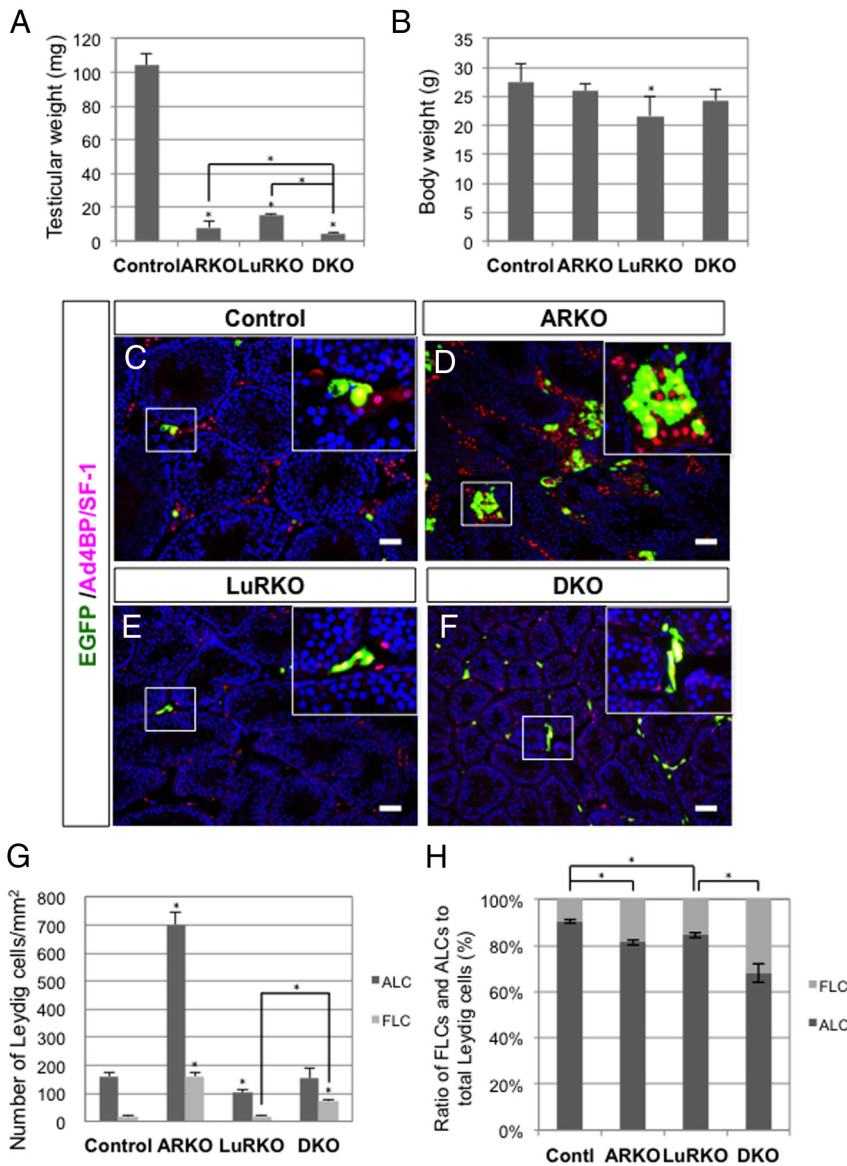
Additionally, the expressions of the *Ar* and *Lhcgr* genes encoding AR and LuR, respectively, was examined at the mRNA level. Total RNA isolated from FLCs and ALCs was subjected to qRT-PCR. As shown in Figure 2E, *Ar* was not expressed in FLCs at E18.5, but then rapidly increased until P10. Thereafter, *Ar* expression continued at a high level at P21 and P56. These results are consistent with the results of the immunofluorescence analyses described above. Expression of *Lhcgr* was detected in FLCs at E18.5, as reported previously (15), and then gradually decreased in FLCs at postnatal stages, whereas its expression in ALCs was significantly higher than that in FLCs at P56 (Figure 2F).

Figure 3. FLCs and ALCs in ARKO, LuRKO, and AR/LuR-DKO mice. A and B, Testicular weights (A) and body weights (B) of control (n = 7), ARKO (n = 8), LuRKO (n = 5), and AR/LuR-DKO (n = 6) mice. *, $P < .05$, significant difference. C–F, *mFLE-EGFP* mice were crossed with ARKO, LuRKO, and DKO mice to analyze the behaviors of FLCs and ALCs in each background. The testes were collected at P56 and subjected to immunofluorescence analyses with antibodies against EGFP (green) and Ad4BP/SF-1 (red). Representative images are shown. The areas in the open rectangles were enlarged and are shown as insets. Scale bars, 50 μm. G, EGFP-positive cells (FLCs) and EGFP-negative cells (ALCs) in control, ARKO, LuRKO, and DKO testes (n = 3 for each) were counted in the sections, and the cell numbers per unit area were plotted as mean ± SEM. *, $P < .05$, significant difference. H, The ratios of FLCs and ALCs were calculated and plotted as mean ± SEM. *, $P < .05$, significant difference.

Postnatal FLCs in ARKO, LuRKO, and DKO mouse testes

It was previously reported that postnatal testis development was severely affected in both ARKO mice (12, 13) and LuRKO mice (15, 17, 19). In fact, the testicular weights in ARKO and LuRKO mice at P56 were significantly lower than that in wild-type mice (Figure 3A). Moreover, the testicular weight of DKO mice was significantly lower than those in ARKO and LuRKO mice. The body weight of LuRKO mice was slightly lower than that of wild-type mice, whereas those of ARKO and DKO mice did not differ significantly from that of wild-type mice (Figure 3B).

Previous observations suggested that both androgen signaling and LH signaling are important for postnatal Leydig cell development. Leydig cells appeared to be hyperplastic, but functionally immature, in ARKO mice (13), whereas small numbers of hypotrophic Leydig cells were observed in the testis of LHβKO mice (14) and LuRKO mice (17, 19, 30). However, there have been no ways to distinguish FLCs from ALCs in the adult testis, and it remains to be clarified whether FLCs and ALCs are distinctively affected by these gene disruptions. To investigate this issue, we generated ARKO mice harboring the *mFLE-EGFP* transgene. Given that EGFP is expressed in an FLC-specific manner in *mFLE-EGFP* mice, we considered EGFP(+)/Ad4BP/SF-1(+) cells as FLCs and EGFP(−)/Ad4BP/SF-1(+) interstitial cells as ALCs.

The testes were collected from ARKO mice and control mice at P56, and stained with antibodies against EGFP and Ad4BP/SF-1. The numbers of FLCs and ALCs were counted on the sections, and the cell numbers per unit area were calculated. As we described previously (4), small numbers of FLCs were observed in the control testis, whereas ALCs predominantly occupied the interstitial space (Figure 3C). The ratio of FLCs to total Leydig cells was approximately 10% in the control testis (Figure 3, G and H). Consistent with previous reports (12, 13), the Leydig cells appeared to be hyperplastic in the ARKO testis (Figure 3D). Both FLCs and ALCs were present in the ARKO testis, and the ratio of FLCs to total Leydig cells was significantly larger than that in the control testis (Figure 3, G and H).

It was reported that postnatal Leydig cell development is dependent on LH (14, 15, 17, 19, 30). Moreover, ARKO mice showed an 8-fold increase in the serum LH concentration (12). Therefore, we investigated the effects of LH signal depletion on postnatal FLCs and ALCs by analyzing LuRKO mice and AR/LuR-DKO mice. The

LuRKO testis has been described to be significantly smaller than the wild-type testis and to contain smaller numbers of Leydig cells (15, 17). These phenotypes were confirmed in the present study. Similar to ARKO mice, both FLCs and ALCs were present in the LuRKO testis. However, both FLCs and ALCs in the LuRKO testis contained small volumes of cytoplasm, suggesting that they were functionally immature (Figure 3E). The density of ALCs was significantly decreased, whereas FLCs seemed unaffected, in the LuRKO testis (Figure 3G). Correspondingly, the numerical ratio of FLCs to total Leydig cells was significantly increased in the LuRKO testis (Figure 3H). These data suggested that ALC development is more severely affected by LH signal depletion than postnatal FLCs. The differential effects of LuR disruption on FLCs and ALCs might be explained by the different expression levels of LuR in postnatal FLCs and ALCs (Figure 2F). Finally, both FLCs and ALC were observed in the DKO testis, and the FLCs in the DKO testis appeared to be hypotrophic, to a similar extent to those in the LuRKO t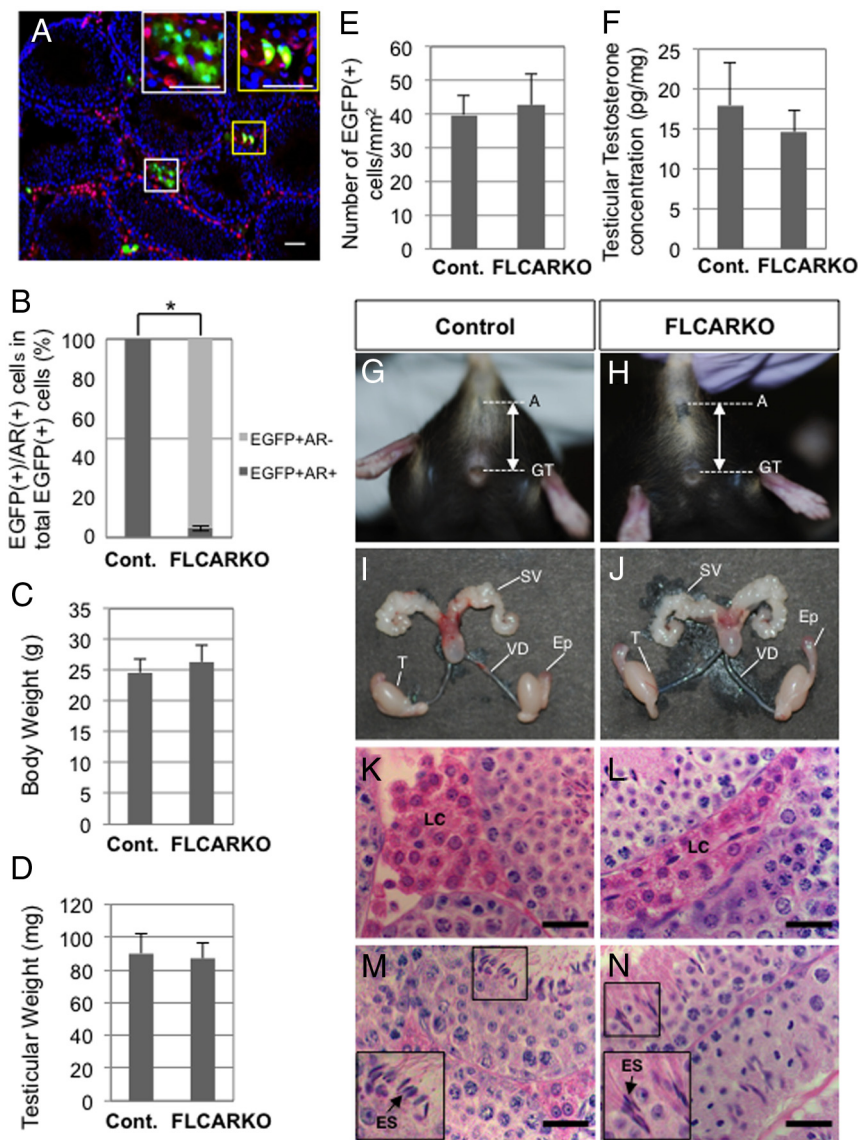estis. The FLC density was significantly higher in the DKO testis than in the LuRKO testis (Figure 3G), and the numerical ratio of FLCs to total Leydig cells (~30%) was also significantly higher in the DKO testis than in the LuRKO testis (Figure 3H). All of these data supported the notion that androgen signaling plays important roles in the regulation of ALC development numerically, whereas FLCs are not significantly affected by androgen signal depletion. To confirm this hypothesis, we further evaluated the effects of FLC-specific androgen signal depletion.

Establishment of an FLC-specific Cre line

To disrupt the *Ar* gene in FLCs, FLC-specific *Cre* mice were generated using the transgenic construct *mFLE-Cre* (Figure 4A). These *Cre* mice were crossed with *CAG-CAT-EGFP* mice (21), and EGFP expression was detected by immunofluorescence analyses. The EGFP signals almost completely overlapped with the interstitial Ad4BP/SF-1 signals at E15.5 (Figure 4B), indicating that *Cre* expression was efficiently and specifically induced in FLCs. On the
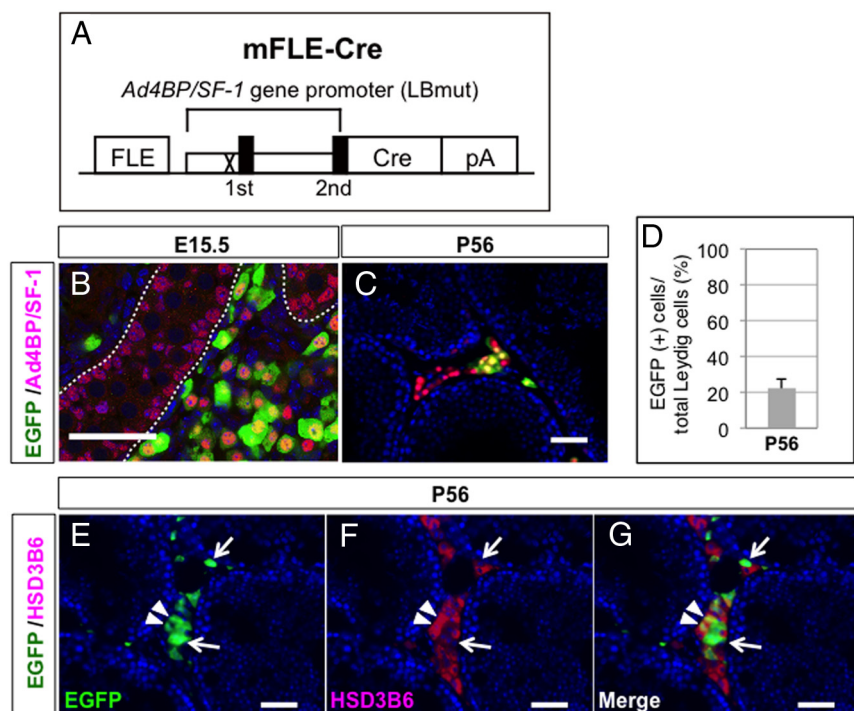
Figure 4. Generation of FLC-specific Cre mice. A, Schematic diagram of the transgenic construct, *mFLE-Cre*, designed to express *Cre* specifically in FLCs. An LHX9-binding site in the proximal promoter of the *Ad4BP/SF-1* gene was mutated (X). The closed boxes indicate the first and second exons. pA, poly(A) signal. B and C, The testes of *mFLE-Cre;CAG-CAT-EGFP* double-transgenic mice were collected at E15.5 (B) and P56 (C) and subjected to immunofluorescence analyses with antibodies against EGFP (green) and Ad4BP/SF-1 (red). The broken lines in B indicate the borders between the testis cord and the interstitial space. D, Ratio of EGFP-positive cells to total Leydig cells in P56 testes (n = 3). E–G, The testes of *mFLE-Cre;CAG-CAT-EGFP* double-transgenic mice were collected and subjected to double immunofluorescence staining of EGFP (green) and HSD3B6 (red). EGFP signals (E), HSD3B6 signals (F), and a merged image (G) are shown. Arrows indicate EGFP(+) and HSD3B6(−) cells, whereas arrowheads indicate EGFP(+) and HSD3B6(+) cells. Scale bars, 50 μm.

other hand, comparisons of the EGFP signals and interstitial Ad4BP/SF-1 signals revealed that only a part of the Leydig cells were immunolabeled for EGFP at the adult stage (Figure 4C). EGFP-positive Leydig cells comprised about 20% of the total Leydig cells in the adult testis (Figure 4D), which was 2-fold greater than the level of EGFP-positive cells in the *mFLE-EGFP* testis. These data suggested that Cre-mediated EGFP expression was induced not only in postnatal FLCs but also in a small part of ALCs. In fact, approximately half of the EGFP-positive cells were HSD3B6-negative (Figure 4, E–G, arrows), whereas the remaining EGFP-positive cells were HSD3B6-positive (Figure 4, E–G, arrowheads). Although Cre-mediated recombination was induced in a small portion of ALCs (less than 10% of total ALCs), the EGFP-positive cell population included almost all of the postnatal FLCs. Therefore, we chose to use these *Cre* mice in the next experiments to evaluate the effects of *Ar* gene disruption in postnatal FLCs.

Effect of FLC-specific AR gene disruption on development of the reproductive tissues

To clarify the cell-autonomous effects of AR disruption in postnatal FLCs, we generated FLCARKO mice by mating *mFLE-Cre* mice with AR-flox mice (23). Initially, the efficiency of *Ar* gene disruption in FLCs was examined by comparing Cre-mediated EGFP expression with AR expression in the adult testis. As previously shown in Figure 2, AR was expressed in all FLCs in the adult testis of wild-type mice. As expected, the AR signals disappeared from most the EGFP-positive cells in the FLCARKO testis, whereas the AR signals in the EGFP-negative cells and Sertoli cells were unaffected (Figure 5A). Cell counting

Figure 5. Phenotypes of FLCARKO mice at P56. A, FLCARKO mice harboring the *CAG-CAT-EGFP* transgene were generated, and P56 testes were subjected to immunofluorescence analyses with antibodies against EGFP (green) and AR (red). The areas in the white and yellow rectangles were enlarged to show EGFP(+)/AR(−) cells and EGFP(+)/AR(+) cells, respectively, in the insets. B, The ratios of EGFP(+)/AR(−) cells to EGFP(+)/AR(+) cells in control (*mFLE-Cre;CAG-CAT-EGFP*) mice (n = 4) and FLCARKO mice harboring the *CAG-CAT-EGFP* transgene (n = 4) were calculated and plotted as mean ± SEM. *, $P < .05$, significant difference. C, The body weights were measured in control mice (n = 15) and FLCARKO mice (n = 11) and plotted as mean ± SEM. D, The testicular weights were measured in control mice (n = 30) and FLCARKO mice (n = 22) and plotted as mean ± SEM. E, The numbers of EGFP-positive cells in control mice and FLCARKO mice harboring the *CAG-CAT-EGFP* transgene (n = 4 for each) were counted, and the cell numbers per unit area were plotted as mean ± SEM (control, 39.8 ± 5.8; FLCARKO, 42.7 ± 9.5). F, The testicular testosterone concentrations in control mice and FLCARKO mice (n = 3 for each) were determined by LC-MS/MS analyses and plotted as mean ± SEM. G and H, Representative photos showing the external genitalia of control mice (G) and FLCARKO mice (H). Bidirectional arrows indicate anogenital distances. A, anus; GT, genital tubercle. I and J, Representative photos showing the internal genitalia of control mice (I) and FLCARKO mice (J). Ep, epididymis; SV, seminal vesicle; T, testis; VD, vas deferens. K–N, Control testes (K and M) and FLCARKO testes (L and N) were collected at P56 and subjected to H&E staining to show the histological features of the interstitial space (K and L) and seminiferous tubules (M and N). Small areas in M and N were enlarged to show the elongated spermatids (ESs) (arrows) in the insets. LC, Leydig cell. Scale bars, 50 μm.

analyses indicated that *Ar* gene disruption was successfully induced in approximately 95% of the EGFP-positive cells (Figure 5B).

The body weight and testicular weight of FLCARKO mice did not differ significantly from those of wild-type mice (Figure 5, C and D). The numbers of EGFP-positive cells were similar between the wild-type and FLCARKO testes (Figure 5E), and the concentrations of intratesticular testosterone were also similar (Figure 5F). Morphologically, the external genitalia and anogenital distance of FLCARKO mice did not differ from those of wild-type male mice (Figure 5, G and H). Internal reproductive tissues such as the testis, seminal vesicle, epididymis, and vas deferens developed normally in FLCARKO mice (Figure 5, I and J). H&E staining of testicular sections revealed normal Leydig cells and spermatogenesis in FLCARKO mice (Figure 5, K–N). These results strongly suggested that the testis of FLCARKO mice is functionally unaffected. To confirm this notion, the reproductive performance of FLCARKO male mice was evaluated at P56 and P105 by 3 consecutive matings with wild-type C57BL/6 female mice. As summarized in Table 1, the FLCARKO male mice successfully produced pups and the litter sizes were comparable with those of wild-type male mice, indicating that reproductive activity was intact in FLCARKO mice.

Effect of FLC-specific AR gene disruption on marker gene expression

Finally, we examined whether marker gene expression was affected in the FLCARKO testis by performing immunofluorescence analyses with antibodies against Ad4BP/SF-1, HSD3B, SRY (Sex determining region Y)-box 9 (SOX9), HSD3B6, HSD17B3, and EGFP. Ad4BP/SF-1 was expressed in both the EGFP-positive and EGFP-negative Leydig cells in the control testis (Figure 6A), and the expression patterns of EGFP and Ad4BP/SF-1 appeared unaffected in the FLCARKO testis (Figure 6B). HSD3B was also expressed in both EGFP-positive and EGFP-negative Leydig cells in the control testis (Figure 6C), and the expression pattern was unaffected in the FLCARKO testis (Figure 6D). SOX9 was expressed in Sertoli cells, and no obvious differences were observed in the intensity or distribution of SOX9 signals between the control (Figure 6E) and FLCARKO (Figure 6F) testes. Cre-mediated EGFP expression was induced in both HSD3B6-negative FLCs (Figure 6G) and HSD3B6-positive ALCs (Figure 6H) in the control testis. We initially estimated that half of the EGFP-positive cells were ALCs (Figure 4, E–G). Subsequent cell counting analyses confirmed our estimation and revealed that about half of the EGFP-positive cells were HSD3B6-positive ALCs (Figure 6J). Interestingly, EGFP/HSD3B6-double-positive cells almost completely disappeared in the FLCARKO testis (Figure 6, I and J), suggesting that HSD3B6 expression was diminished in EGFP-labeled ALCs because of cell-autonomous androgen signal depletion. We further analyzed the expression pattern of another ALC marker protein, HSD17B3, and confirmed that HSD17B3 expression also disappeared in EGFP-labeled ALCs (Supplemental Figure 6). Taken together, the androgen signal depletion in FLCs did not affect marker gene expression, whereas unintended AR disruption in a small part of ALCs resulted in the disappearance of HSD3B6 and HSD17B3 expressions in these cells.
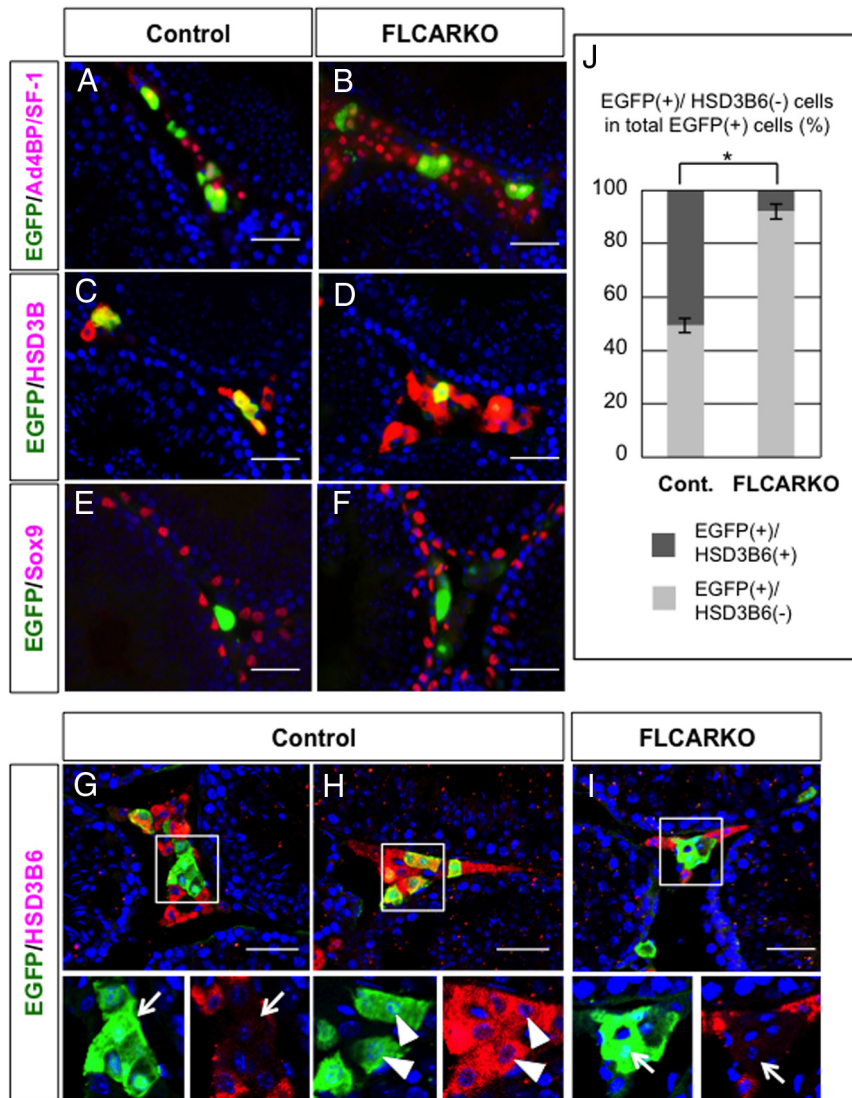
Discussion

It has long been believed that FLCs are completely replaced by ALCs soon after birth in rodents (1, 2, 6–9). However, a few researchers have argued for the persistence of FLCs in the postnatal testis based on morphological analyses (10, 11). The present study has provided a definitive answer to this question, namely that FLCs and/or their descendants persist in the adult testis in mice. Postnatal FLCs were characterized as an HSD3B6-negative and HSD17B3-negative Leydig subpopulation, and they coexisted with mature ALCs expressing both HSD3B6 and HSD17B3. According to a previous stereological study, the number of FLCs is about 5×10^4 at P1, whereas the number of total Leydig cells is about 150×10^4 at adult stage (31). Given that EGFP-positive FLCs

Table 1. Fertility of Control Mice and FLCARKO Mice at P56 and P105

| | Number of Pups | | | |
	1st	2nd	3rd	Average
P56				
Control	5	7	9	7.0
	7	7	8	7.3
	NP	9	NP	9.0
				7.7 ± 1.1
FLCARKO	8	7	5	6.7
	7	5	6	6.0
	8	6	7	7.0
				6.6 ± 0.5
P105				
Control	8	8	8	8.0
	8	6	7	7.0
	8	7	8	7.7
				7.6 ± 0.5
FLCARKO	7	8	6	7.0
	8	NP	9	8.5
	7	8	9	8.0
				7.8 ± 0.4

Numbers of pups delivered by females mated with control or FLCARKO male at P56 and P105. Data are shown as mean ± SEM. NP, not pregnant.

Figure 6. Testicular marker gene expressions in FLCARKO mice. A–F, Testes were collected from control (*mFLE-Cre;CAG-CAT-EGFP*) mice (A, C, and E) and FLCARKO mice harboring the *CAG-CAT-EGFP* transgene (B, D, and F) and subjected to immunofluorescence analyses with antibodies against EGFP (green) and Ad4BP/SF-1 (red) (A and B), EGFP (green) and HSD3B (red) (C and D), or EGFP (green) and SOX9 (red) (E and F). G and H, Control testes were collected and subjected to immunofluorescence analyses with antibodies against EGFP (green) and HSD3B (red). The areas enclosed by the rectangles were enlarged, and the signals in each channel are shown in the small panels. Most of the EGFP(+) and HSD3B6(−) cells form small clusters (arrows) (G), whereas considerable numbers of EGFP(+) and HSD3B6(+) cells are sparsely distributed in the interstitium (arrowheads) (H). I, Testes collected from FLCARKO mice harboring the *CAG-CAT-EGFP* transgene were subjected to the same analyses. Almost all EGFP(+) cells are HSD3B6-negative, as indicated by the arrows in the small panels. Scale bars, 50 μm. J, The ratios between EGFP(+)/HSD3B6(+) and EGFP(+)/HSD3B6(−) cells in control testes and FLCARKO testes at P56 were calculated and shown as mean ± SEM. *, $P < .05$, significant difference between the samples.

Recent studies have provided novel insights into the origins of FLCs and ALCs. One suggested that FLCs and ALCs share a common progenitor pool in the fetal testis (32), whereas others insisted that a part of the interstitial cells in the fetal testis are already determined to develop into ALCs (28, 33). Although the origins of FLCs and ALCs remain obscure, it is generally accepted that functionally differentiated FLCs do not contribute to the ALC population (1, 2, 7, 8, 32). In support of this assumption, our lineage-tracing experiments demonstrated that FLCs hardly contributed to the HSD3B6/HSD17B3-positive ALC population at the adult stage. On the other hand, *mFLE-Cre* induced EGFP expression not only in FLCs but also in a small part of ALCs. These results leave open the possibility that a part of FLCs transdifferentiated into ALCs. This possibility should be further investigated in future studies.

In the ARKO testis, Leydig cells become hyperplastic but do not express HSD3B6 and HSD17B3. Because FLCs have been believed to disappear from the postnatal testis, the Leydig cells in the ARKO testis were considered to be immature ALCs (13). However, our data indicated that FLCs persist in the adult testis of wild-type mice, raising the question of whether FLCs or ALCs are predominantly localized in the ARKO testis. In the present study, we generated ARKO mice in which FLCs are labeled with EGFP and demonstrated that both FLCs and ALCs persist in the ARKO testis. The ratio of ALCs to total Leydig

were approximately 10% of total Leydig cells, it was estimated that FLCs increased only about 3-fold in 8 weeks. Because ALCs appeared and rapidly increased in the postnatal testis, FLCs could occupy only a small percentage of the total Leydig cells in the adult testis. In support of this notion, our data indicated that FLCs are not actively proliferating both at fetal and adult stages.

cells was about 90% in the control testis and decreased to about 80% in the ARKO testis. Furthermore, the ratio of ALCs was more than 80% in the LuRKO testis and decreased to less than 70% in the AR/LuR-DKO testis. Given that previous studies revealed that the total Leydig cell number is decreased in ARKO mice (12, 13), the decline in the ALC population in the ARKO and DKO

testes strongly suggested that androgen signaling is involved in the regulation of the ALC number. In support of this notion, it was previously reported that androgen signaling induces the differentiation of ALC precursors into immature ALCs (34).

The phenotypes in ARKO mice suggest that activation of AR is essential for ALC maturation (13). However, AR is expressed in a variety of cell types in the testis, and thus the testicular phenotype in ARKO mice is a summation of the effects on multiple cell types. In fact, recent studies clarified that androgen signaling in Sertoli cells (12, 35–37) and peritubular myoid cells (38, 39) is essential for Leydig cell development. Therefore, it has been an important task to clarify the cell-autonomous function of androgen signaling in Leydig cells. In a previous study, anti-Mullerian hormone receptor 2-Cre (*Ambr2-Cre*) mice were used to generate Leydig cell-specific ARKO mice (40). However, *Ambr2-Cre* could not achieve complete AR disruption in all Leydig cells, and induced AR disruption not only in Leydig cells but also in some Sertoli cells. Therefore, the cell-autonomous action of AR in Leydig cells has remained inconclusive. More recently, another Leydig cell-specific ARKO model was generated by using fatty acid binding protein 4 (*Fabp4*)-*Cre* mice (41). Although AR disruption was also incomplete (~75%) in these mice, the results of this study strongly suggested that cell-autonomous AR action is essential for ALC maturation. In the present study, we succeeded in generating mice with *Cre* expression under the control of an FLE (*mFLE-Cre* mice), and these mice enabled us to generate FLCARKO mice. FLCARKO mice showed normal testosterone levels and normal fertility, strongly suggesting that androgen signaling in FLCs is dispensable for male reproductive functions. Unexpectedly, *mFLE-Cre* induced *Cre* expression not only in FLCs but also in a small number of ALCs. In these ALCs, AR disruption led to loss of HSD3B6 and HSD17B3 expressions, supporting the notion that AR regulates HSD3B6 and HSD17B3 expressions in ALCs in a cell-autonomous manner. Recently, FLC lineage-specific *Ar* gene disruption was achieved using retinoic acid receptor β-Cre (*Rarb-Cre*) mice (28). These mice showed phenotypes that were largely different from those in our FLCARKO mice, such as late-onset infertility, incomplete differentiation of ALCs, and abnormal accumulation of lipid droplets in Leydig cells of aged mice. A major difference between our study and the previous study is that we induced *Cre* expression only in differentiated FLCs, whereas *Rarb-Cre* labeled FLCs as well as presumptive FLC precursors. Because a recent study suggested functional interplay between FLC precursors

and ALC precursors in the fetal testis (32), it is possible that AR disruption in FLC precursors induced dysfunction of ALC precursors, resulting in abnormal ALC development. Another possibility is that *Rarb-Cre* induced AR disruption not only in the FLC lineage but also in a part of the ALC precursors. AR disruption in a substantial number of ALCs might impair the reproductive functions of the KO mice.

Our study has definitively demonstrated that FLCs persist after birth and raises a fundamental question as to whether postnatal FLCs are functionally important. Postnatal FLCs do not express HSD17B3, and thus cannot synthesize testosterone. Therefore, the functional importance of postnatal FLCs, if any, cannot be explained by our current knowledge about Leydig cell functions. One of the intriguing findings in the present study is that FLCs express AR only in the postnatal stages, and not in the prenatal stages, suggesting that FLCs change their characteristics during development. Transcriptomic analyses of FLCs at various developmental stages will provide clues toward the stage-specific functions of postnatal FLCs. In addition, to fully elucidate the functional importance of the postnatal FLC population, more effective methods, such as toxin-mediated cell ablation experiments or FLC-specific *Ad4BP/SF-1* (*Nr5a1*) gene disruption, will be required in future studies.

In the present study, we have clearly revealed that FLCs persist in the postnatal testis. Moreover, we deleted one of the most important signaling pathways in Leydig cell development, androgen signaling, in postnatal FLCs. However, the number of FLCs was unchanged and gene expression pattern in FLCs appeared to be unaffected, strongly suggesting that postnatal FLCs are an androgen-independent cell population. Our study provides novel insights into Leydig cell development, and we believe that it will be a starting point to advance our understanding of the nature and biological importance of FLCs at postnatal stages.

References

1. **Habert R, Lejeune H, Saez JM.** Origin, differentiation and regulation of fetal and adult Leydig cells. *Mol Cell Endocrinol*. 2001;179:47–74.

2. **Haider SG.** Cell biology of Leydig cells in the testis. *Int Rev Cytol*. 2004;233:181–241.

3. **O'Shaughnessy PJ, Baker PJ, Heikkilä M, Vainio S, McMahon AP.** Localization of 17β-hydroxysteroid dehydrogenase/17-ketosteroid reductase isoform expression in the developing mouse testis–androstenedione is the major androgen secreted by fetal/neonatal leydig cells. *Endocrinology*. 2000;141:2631–2637.

4. **Shima Y, Miyabayashi K, Haraguchi S, et al.** Contribution of Leydig and Sertoli cells to testosterone production in mouse fetal testes. *Mol Endocrinol*. 2013;27:63–73.

5. **O'Shaughnessy PJ, Willerton L, Baker PJ.** Changes in Leydig cell gene expression during development in the mouse. *Biol Reprod*. 2002;66:966–975.

6. **O'Shaughnessy PJ, Baker PJ, Johnston H.** The foetal Leydig cell–differentiation, function and regulation. *Int J Androl*. 2006;29:90–95; discussion 105–108.

7. **Griswold SL, Behringer RR.** Fetal Leydig cell origin and development. *Sex Dev*. 2009;3:1–15.

8. **Svingen T, Koopman P.** Building the mammalian testis: origins, differentiation, and assembly of the component cell populations. *Genes Dev*. 2013;27:2409–2426.

9. **Teerds KJ, Huhtaniemi IT.** Morphological and functional maturation of Leydig cells: from rodent models to primates. *Hum Reprod Update*. 2015;21:310–328.

10. **Ariyaratne HB, Chamindrani Mendis-Handagama S.** Changes in the testis interstitium of Sprague Dawley rats from birth to sexual maturity. *Biol Reprod*. 2000;62:680–690.

11. **Kerr JB, Knell CM.** The fate of fetal Leydig cells during the development of the fetal and postnatal rat testis. *Development*. 1988;103:535–544.

12. **De Gendt K, Atanassova N, Tan KA, et al.** Development and function of the adult generation of Leydig cells in mice with Sertoli cell-selective or total ablation of the androgen receptor. *Endocrinology*. 2005;146:4117–4126.

13. **O'Shaughnessy PJ, Johnston H, Willerton L, Baker PJ.** Failure of normal adult Leydig cell development in androgen-receptor-deficient mice. *J Cell Sci*. 2002;115:3491–3496.

14. **Ma X, Dong Y, Matzuk MM, Kumar TR.** Targeted disruption of luteinizing hormone β-subunit leads to hypogonadism, defects in gonadal steroidogenesis, and infertility. *Proc Natl Acad Sci USA*. 2004;101:17294–17299.

15. **O'Shaughnessy PJ, Baker P, Sohnius U, Haavisto AM, Charlton HM, Huhtaniemi I.** Fetal development of Leydig cell activity in the mouse is independent of pituitary gonadotroph function. *Endocrinology*. 1998;139:1141–1146.

16. **Pointis G, Mahoudeau JA.** Responsiveness of foetal mouse testis to gonadotrophins at various times during sexual differentiation. *J Endocrinol*. 1977;74:149–150.

17. **Zhang FP, Poutanen M, Wilbertz J, Huhtaniemi I.** Normal prenatal but arrested postnatal sexual development of luteinizing hormone receptor knockout (LuRKO) mice. *Mol Endocrinol*. 2001;15:172–183.

18. **O'Shaughnessy PJ, Fowler PA.** Endocrinology of the mammalian fetal testis. *Reproduction*. 2011;141:37–46.

19. **Lei ZM, Mishra S, Zou W, et al.** Targeted disruption of luteinizing hormone/human chorionic gonadotropin receptor gene. *Mol Endocrinol*. 2001;15:184–200.

20. **Shima Y, Miyabayashi K, Baba T, et al.** Identification of an enhancer in the Ad4BP/SF-1 gene specific for fetal Leydig cells. *Endocrinology*. 2012;153:417–425.

21. **Kawamoto S, Niwa H, Tashiro F, et al.** A novel reporter mouse strain that expresses enhanced green fluorescent protein upon Cre-mediated recombination. *FEBS Lett*. 2000;470:263–268.

22. **Sato T, Matsumoto T, Yamada T, Watanabe T, Kawano H, Kato S.** Late onset of obesity in male androgen receptor-deficient (AR KO) mice. *Biochem Biophys Res Commun*. 2003;300:167–171.

23. **Kawano H, Sato T, Yamada T, et al.** Suppressive function of androgen receptor in bone resorption. *Proc Natl Acad Sci USA*. 2003;100:9416–9421.

24. **Shima Y, Zubair M, Komatsu T, et al.** Pituitary homeobox 2 regulates adrenal4 binding protein/steroidogenic factor-1 gene transcription in the pituitary gonadotrope through interaction with the intronic enhancer. *Mol Endocrinol*. 2008;22:1633–1646.

25. **Fatchiyah, Zubair M, Shima Y, et al.** Differential gene dosage effects of Ad4BP/SF-1 on target tissue development. *Biochem Biophys Res Commun*. 2006;341:1036–1045.

26. **Yamamura K, Doi M, Hayashi H, et al.** Immunolocalization of murine type VI 3β-hydroxysteroid dehydrogenase in the adrenal gland, testis, skin, and placenta. *Mol Cell Endocrinol*. 2014;382:131–138.

27. **Majdic G, Millar MR, Saunders PT.** Immunolocalisation of androgen receptor to interstitial cells in fetal rat testes and to mesenchymal and epithelial cells of associated ducts. *J Endocrinol*. 1995;147:285–293.

28. **Kaftanovskaya EM, Lopez C, Ferguson L, Myhr C, Agoulnik AI.** Genetic ablation of androgen receptor signaling in fetal Leydig cell lineage affects Leydig cell functions in adult testis. *FASEB J*. 2015;29:2327–2337.

29. **Zhou X, Kudo A, Kawakami H, Hirano H.** Immunohistochemical localization of androgen receptor in mouse testicular germ cells during fetal and postnatal development. *Anat Rec*. 1996;245:509–518.

30. **Zhang FP, Pakarainen T, Zhu F, Poutanen M, Huhtaniemi I.** Molecular characterization of postnatal development of testicular steroidogenesis in luteinizing hormone receptor knockout mice. *Endocrinology*. 2004;145:1453–1463.

31. **O'Shaughnessy PJ, Monteiro A, Abel M.** Testicular development in mice lacking receptors for follicle stimulating hormone and androgen. *PLoS One*. 2012;7:e35136.

32. **Barsoum IB, Kaur J, Ge RS, Cooke PS, Yao HH.** Dynamic changes in fetal Leydig cell populations influence adult Leydig cell populations in mice. *FASEB J*. 2013;27:2657–2666.

33. **Kilcoyne KR, Smith LB, Atanassova N, et al.** Fetal programming of adult Leydig cell function by androgenic effects on stem/progenitor cells. *Proc Natl Acad Sci USA*. 2014;111:E1924–E1932.

34. **Hardy MP, Kelce WR, Klinefelter GR, Ewing LL.** Differentiation of Leydig cell precursors in vitro: a role for androgen. *Endocrinology*. 1990;127:488–490.

35. **Hazra R, Jimenez M, Desai R, Handelsman DJ, Allan CM.** Sertoli cell androgen receptor expression regulates temporal fetal and adult Leydig cell differentiation, function, and population size. *Endocrinology*. 2013;154:3410–3422.

36. **Rebourcet D, O'Shaughnessy PJ, Monteiro A, et al.** Sertoli cells maintain Leydig cell number and peritubular myoid cell activity in the adult mouse testis. *PLoS One*. 2014;9:e105687.

37. **Rebourcet D, O'Shaughnessy PJ, Pitetti JL, et al.** Sertoli cells control peritubular myoid cell fate and support adult Leydig cell development in the prepubertal testis. *Development*. 2014;141:2139–2149.

38. **Welsh M, Saunders PT, Atanassova N, Sharpe RM, Smith LB.** Androgen action via testicular peritubular myoid cells is essential for male fertility. *FASEB J*. 2009;23:4218–4230.

39. **Welsh M, Moffat L, Belling K, et al.** Androgen receptor signalling in peritubular myoid cells is essential for normal differentiation and function of adult Leydig cells. *Int J Androl*. 2012;35:25–40.

40. **Xu Q, Lin HY, Yeh SD, et al.** Infertility with defective spermatogenesis and steroidogenesis in male mice lacking androgen receptor in Leydig cells. *Endocrine*. 2007;32:96–106.

41. **O'Hara L, McInnes K, Simitsidellis I, et al.** Autocrine androgen action is essential for Leydig cell maturation and function, and protects against late-onset Leydig cell apoptosis in both mice and men. *FASEB J*. 2015;29:894–910.